The Space Congress® Proceedings

1995 (32nd) People and Technology - The Case For Space

Apr 27th, 1:00 PM - 4:00 PM

Paper Session III-A - Dual-Use Applications of a Computational Fluid Dynamics Code for Viscous Incompressible Flow

Cetin Kiris
NASA Ames Research

Dochan Kwak
NASA Ames Research

Stuart E. Rogers
NASA Ames Research

Follow this and additional works at: https://commons.erau.edu/space-congress-proceedings

Scholarly Commons Citation

EMBRY-RIDDLE
Aeronautical University™
SCHOLARLY COMMONS

DUAL-USE APPLICATIONS OF A COMPUTATIONAL FLUID DYNAMICS CODE FOR VISCOUS INCOMPRESSIBLE FLOW

Cetin Kiris*, Dochan Kwak, Stuart E. Rogers
NASA Ames Research Center, M.S.T27B-1
Moffett Field, CA 94035

Abstract

An efficient incompressible flow analysis code, INS3D, has been developed at NASA Ames Research Center and applied successfully to numerous aerospace applications. The INS3D code has also been applied to non-aerospace applications, such as biofluid problems, with great success. This paper presents a computational flow simulation capability originally developed for liquid rocket engine analysis and subsequently applied to analyze the left ventricular assist device being developed jointly by NASA Johnson Space Center and the Baylor College of Medicine.

1. Introduction

Computational fluid dynamics has been developed to a level where it has become an indispensable part of aerospace research and design. Advanced component systems in the next generation of transport vehicles, such as advanced liquid rocket engine fuel systems, marine propulsion systems, and aircraft high-lift configurations, are likely to require more efficient and simpler designs with lower manufacturing costs. Fast and reliable incompressible flow simulation capabilities are crucial to developing these new designs. For example, in order to understand the source of the noise generated by a high-lift wing-flap system, the unsteady flowfield around these configurations must be resolved accurately. A second example of a viscous incompressible flowfield is the rotor-stator interaction in turbomachinery. A flange-to-flange rocket engine fuel-pump simulation must account for the interaction between the rotating and non-rotating components: the flow straighteners, the impeller, the volute and diffusers. A Ventricular Assist Device (VAD) developed by NASA Johnson Space Center (JSC) and Baylor College of Medicine (BCOM) has a design similar to a rocket engine fuel pump in that it also consists of a flow straightener, an impeller, and a diffuser.[1] Such incompressible flow simulation capability can be beneficial to the development of artificial heart devices. Technology developed for aerospace applications can also be utilized for the benefit of human health. Accurate and detailed knowledge of the flowfield obtained by steady and unsteady incompressible flow calculations can be greatly beneficial to designers in their effort to reduce the cost and improve the reliability of these devices.

Analysis of biofluid flow problems are challenging and the potential impact of an advanced computational tool on medical research for improving health care is enormous. For example, the blood flow through mechanical hearts, heart assist devices, and heart valves is unsteady and involves moving walls making experimental study very difficult. Computational analysis offers an alternative to experimental methods which can produce flow field data in great detail. Medical researchers can study this extensive data to obtain a better understanding of the flow physics. Computational analysis can also be used to optimize the design of mechanical devices at a significantly lower cost and time than required by an empirical approach.

In addition to the geometric complexities, a variety of flow phenomena are encountered in biofluids. These include turbulent boundary layer separation, wakes, transition, tip vortex resolution, three-dimensional effects, and Reynolds number effects. In order to increase the role of Computational Fluid Dynamics (CFD) in the design process, the CFD analysis tools must be evaluated and validated so that designers gain confidence in their use. The incompressible flow solver, INS3D, has been applied to various viscous flow problems and extensively validated.[2-13] This paper details how the computational flow simulation capability developed for liquid rocket engine pump component analysis has been applied to the Left Ventricular Assist Device being developed jointly by NASA JSC and Baylor College of Medicine.

(*) MCAT Inc.

2. Algorithm

The algorithm used in the INS3D code is based on the method of pseudocompressibility where the time-derivative of pressure is introduced into the continuity equation. The elliptic-parabolic type partial differential equations are transformed into the hyperbolic-parabolic type. Since the convective terms of the resulting equations are hyperbolic, upwind differencing can be applied to these terms. Third- and fifth-order flux-difference splitting is used for the convective terms. The upwind differencing leads to a more diagonal dominant system than does central differencing and does not require any user-specified artificial dissipation. The viscous flux derivatives are computed using central differencing. When the equations are solved in a steady rotating frame of reference, the centrifugal force and the Coriolis force are also added as source terms to the governing equations. In the steady-state formulation, the time derivatives are differenced using the Euler backward formula. The equations are solved iteratively in pseudo-time until the solution converges to a steady state. In the time-accurate formulation, the equations are iterated to convergence in pseudo-time for each physical time step until the divergence of the velocity field is reduced below a specified tolerance value.

Discretization of the governing equations results in a matrix equation that is solved iteratively using a nonfactored Gauss-Seidel type line-relaxation scheme, which maintains stability and allows the use of a large pseudo-time step. Details of the numerical method can be found in Refs. 4-5. The present calculations use the one-equation turbulence model developed by Baldwin and Barth.[14] In this model, the transport equation for the turbulent Reynolds number is derived from a simplified form of the standard $k - \epsilon$ model equations. The model is relatively easy to implement because there is no need to define an algebraic length scale. The transport equation is solved by using the same Gauss-Seidel type line-relaxation scheme as the mean-flow equations.

3. Liquid Rocket Engine Pump Components

Until recently, the high performance pump design process was not significantly different from that of three decades ago. During this time, a vast amount of experimental and operational experience has demonstrated that there are many important features of pump flows that are not accounted for in the current semi-empirical design process. Pumps being designed today are no more technologically advanced than those designed for the Space Shuttle Main Engine (SSME). During that same time span, huge strides have been made in computers, numerical algorithms, and physical modeling. One major accomplishment of this work is to extend CFD technology by validating an advanced CFD code for pump flows and demonstrating their value to pump designers.

The validation effort for pump components has focused on inducers and impellers.[9-10] The computed results from a numerical simulation of the flow through a rocket pump inducer were compared with experimental measurements. The design of an advanced impeller was verified by simulating the flow through the baseline and the optimized geometries. The effects of the vaneless space in the advanced impeller concept were investigated by using the incompressible Navier-Stokes flow simulation capability.[10] The comparisons reported in Ref. 9-10 showed that the computations compared well with experiments. The resulting computational procedure with the one-equation Baldwin-Barth turbulence model was applied to the flow through the SSME High Pressure Fuel Turbo-Pump (HPFTP) impeller. The SSME-HPFTP impeller has 6 full blades, 6 long partial blades, and 12 short partial blades. The impeller wheel speed is 6,300 rpm, and the Reynolds number for this calculation is 181,000 per inch. Figure 1 shows the nondimensional pressure contours on the hub surface of the impeller. Since the pressure rise between the impeller inlet and the exit is quite large, the pressure variations between the suction and the pressure sides of the blades are not noticeable from this figure. This calculation includes the vaneless space between the impeller trailing edge and the diffuser vane leading edge. Figure 2 shows blade-to-blade velocity and flow angle distributions at two stations downstream from the SSME-HPFTP impeller exit. Blade-to-blade velocity distribution illustrates the impeller exit flow distortion. Solid lines represent the experimental data and dashed lines represent computed results. The jet-wake pattern, which produces an unsteady load on the diffuser vanes, was captured at both meridional locations. The numerical results compare reasonably well with the experimental data. The pressure contours in Figure 1 also indicates this jet-wake pattern.

4. Left Ventricular Assist Device

In 1989, NASA Johnson Space Center (JSC) began a joint project with the DeBakey Heart Center of the Baylor College of Medicine (BCOM) in Houston to develop a new implantable LVAD prototype system. This LVAD is based on a fast rotating axial pump requiring a minimum number of moving parts. To make it implantable, the device has been made as small as possible, requiring a very high rotational speed. The computational procedure described above for pump components has been used to provide the designers with a view of the complicated fluid dynamic processes inside this device. Due to the nature of the device, this detailed information cannot be obtained experimentally. The detailed computational look at the fluid flow is very important to the designers; high levels of turbulence can damage the red blood cells and regions of recirculating flow can lead to blood clots. Thus the ability to predict these phenomena can greatly help the designers.

The flow through the baseline design of the LVAD impeller was numerically simulated by solving the incompressible Navier-Stokes equations in a steady rotating frame of reference. Zonal multiblock grids were used in this component analysis. The geometry and the computational grid of the LVAD baseline impeller are shown in Figure 3. The domain is divided into five zones with dimensions of 127 x 39 x 33, 127 x 39 x 33, 59 x 21 x 7, 47 x 21 x 5, and 59 x 21 x 7, respectively. Zone 1 is the region between the suction side of the partial blade and the pressure side of the full blade; the region between the pressure side of the partial blade and the suction side of the full blade is filled by zone 2; and zones 3 through 5 allow tip-leakage effects to be included in the computational study and occupy the regions between the impeller blade tip and the casing. At the zonal interfaces, grid points were matched one-to-one. For all zones, an H-H type grid topology was used. An H-type surface grid was generated for each surface using an elliptic grid generator. The interior region of the three-dimensional grid was filled using an algebraic grid generator coupled with an elliptic smoother. Periodic boundary conditions were used at the end points in the rotational direction. The design flow of this impeller is 5 liters per minute and the design speed is 12,600 revolutions per minute (rpm). The problem was nondimensionalized by the tube diameter (0.488 inches) and the impeller tip velocity. The solution was considered converged when the maximum residual had dropped at least five orders of magnitude. Computer time required per grid point per iteration was about 1.5×10^{-4} seconds. The total computer time required for these calculations was about 6 to 8 single processor Cray-C90 hours. A parametric study was performed to optimize the impeller blade shape and the tip clearance. Initially, three different impeller blade designs with a tip clearance of 0.009 inches were analyzed. Figure 4 shows the axial velocity contours at the exit plane of the impeller for various blade curvatures. Design III shows massive seperation near the suction side of the partial blade trailing edge because of the high curvature blade shape. Design II, which has less blade curvature than design I, shows flow features very similar to design I. Design I was analyzed with two tip clearances; the tip clearance of 0.0045 inches shows better hydrodynamic performance in terms of efficiency and head coefficient than with a tip clearance of 0.009 inches. Using the design I with a tip clearance of 0.0045 inches as the baseline impeller design, ideas from rocket propulsion and medical science were combined to develop a new implantable LVAD. In collaboration with the NASA-JSC engineering team and BCOM researchers, a new design consisting of the baseline impeller plus an inducer was investigated. The hub and blade surfaces of the baseline impeller and the new impeller are colored by nondimensionalized pressure in Figure 5. The pressure is nondimensionalized by ρV^2, where ρ is the density and V is the impeller tip velocity. The pressure gradient across the blades due to the action of centrifugal force, and the pressure rise from inflow to outflow are shown. The table in Figure 5 shows the clinical results obtained by BCOM. Further clinical hemolysis testing and animal implantation by BCOM are currently underway using the new inducer-impeller design. The hemolysis index reported in Figure 5 shows the amount of hemoglobin generated by the pump in grams per 100 liters. Destruction of the red blood cells results in the release of hemoglobin. Red blood cels are damaged due to regions of high shear and separated flows. The new design shows a remarkable improvement in performance over the baseline design. The inducer provides a sufficient pressure rise to the flow in order to prevent the cavitation on the impeller blades. Figure 6 shows the particle traces through the new impeller. The traces are colored by the relative total-velocity magnitude. The particles were released near the inducer leading edge, the hub, the inducer blade pressure side, and the tip regions. The swirling motion of the particles indicates a secondary flow region between the partial and the full blades. The particles released near the pressure side of the blade indicate a radial velocity component inside the blade boundary layer. The particles tend to flow from the hub to the tip of the blade. The particles near the inducer leading edge and full blade trailing edge indicate the presence of a back flow.

In the next step of the design process, this computational analysis tool will be used to improve the

diffuser geometry and the bearing design. This unique insight into the internal fluid structures will lead to improved components for an improved heart assist device. In July 1991, the Institute of Medicine estimated that approximately 25,000 to 60,000 patients per year in North America could benefit from an efficient left ventricular assist device. Thus improved designs made possible because of the current work could have a far reaching impact on human health.

5. Conclusions

An efficient and robust solution technique for 3-D pump component analysis and its spin-off application to an LVAD impeller analysis has been presented. The technique solves the viscous incompressible Navier-Stokes equations with source terms in a steadily rotating reference frame. The method of pseudo-compressibility with higher-order accurate upwind differencing and a Gauss-Seidel line relaxation scheme are utilized. The flow through the SSME-HPFTP impeller has been successfully simulated. Numerical results utilizing the one-equation Baldwin-Barth turbulence model compare fairly well with experimental data. This validated solution procedure has been applied to the NASA JSC/BCOM LVAD impeller. Parametric studies were performed to analyze the performance of the LVAD impeller. Substantial improvements were observed when inducer blades were included upstream of the impeller main blades.

References

1. Aber, G. S., Akkerman, J.W., Bozeman, R. J., and Saucier, D. R., "Development of the NASA / Baylor VAD," NASA Technology 2003 Conference, 1993.

2. Kwak, D., Chang, J. L C., Shanks, S. P., and Chakravarthy, S., "A Three-Dimensional Incompressible Navier-Stokes Flow Solver Using Primitive Variables," *AIAA Journal*, Vol. 24, No. 3, pp. 390-396, 1977.

3. Chang, J., Kwak, D., Rogers, S. E., and Yang, R.-J., "Numerical Simulation Methods of Incompressible Flows and an Application to the Space Shuttle Main Engine," *International Journal of Numerical Methods in Fluids*, Vol 8, pp. 1241-1268, 1988.

4. Rogers, S. E., Kwak, D., "Upwind Differencing for the Time-Accurate Incompressible Navier-Stokes Equations," *AIAA Journal*, Vol. 28, No. 2, pp. 253-262, 1990.

5. Rogers, S. E., Kwak, D. and Kiris, C., "Numerical Solution of the Incompressible Navier-Stokes Equations for Steady and Time-Dependent Problems," *AIAA Journal*, Vol. 29, No. 4, pp. 603-610, 1991.

6. Rogers, S. E., Wiltberger, N. L., and Kwak, D. "Efficient Simulation of Incompressible Viscous Flow Over Single and Multi-Element Airfoils," AIAA Paper No. 92-0405, 1992.

7. Rogers, S. E., "Progress In High-Lift Aerodynamic Calculations," AIAA Paper No. 93-0194, 1993.

8. Rogers, S. E., "A Comparison of Turbulence Models In Computing Multi-Element Airfoil Flows," AIAA Paper No. 94-0291, 1994.

9. Kiris, C., Chang, L., Kwak, D., and Rogers, S. E., "Incompressible Navier-Stokes Computations of Rotating Flows," AIAA Paper No. 93-0678, 1993.

10. Kiris, C. and Kwak, D., "Progress in Incompressible Navier-Stokes Computations for the Analysis of Propulsion Flows," NASA CP 3282, Vol II, Advanced Earth-to-Orbit Propulsion Technology, 1994.

11. Kiris, C. Rogers, S., Kwak, D., and Lee, Y. T., "Time-Accurate Incompressible Navier-Stokes Computations with Overlapped Moving Grids," ASME Fluids Engineering Summer Meeting, Lake Tahoe, Nevada, June 19-23, 1994.

12. Kiris, C., Rogers, S. E., Kwak, D. and Chang, I. "Computation of Incompressible Viscous Flows through Artificial Heart Devices with Moving Boundaries," *Fluid Dynamics in Biology*, Proceedings of an AMS-IMS-SIAM Joint Research Conference, edited by A. Y. Cheer and C. P. van Dam, American Mathematical Society, Providence, R. I., 1991, pp. 237-247.

13. Dacles-Mariani, J., Rogers, S. E., Kwak, D., Zilliac, G., and Chow, J., "A Computational Study of Wingtip Vortex Flowfield," AIAA Paper No. 93-3010, 1993.

14. Baldwin, B., S. and Barth, T., J., "A One-Equation Turbulence Transport Model for Bigh Reynolds Number Wall-Bounded Flows," AIAA Paper No. 91-0610, 1991.

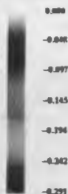# 11 INCH SSME HPFTP IMPELLER

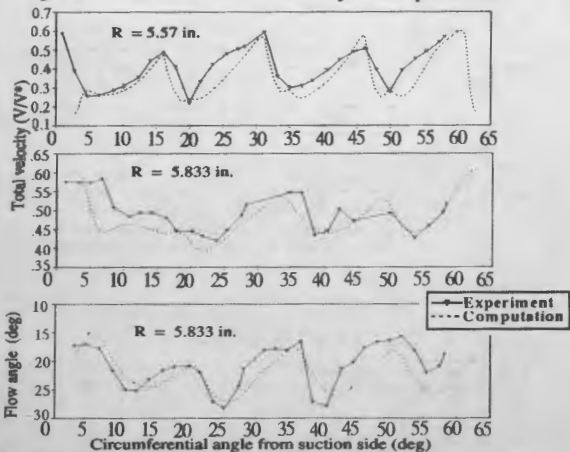*Pressure*

Figure 1 : Hub surface colored by static pressure

Figure 2 : Velocity and flow angle distributions downstream of
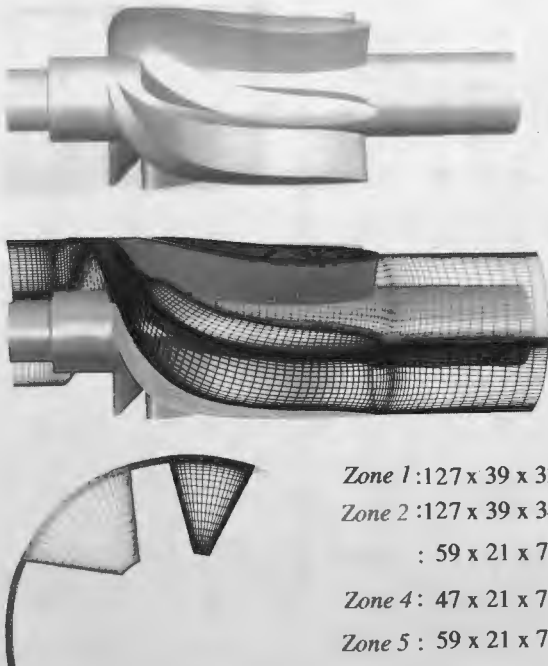SSME-HPFTP impeller exit plane (impeller exit radius : 5.5 in.)

Zone 1 : 127 x 39 x 33
Zone 2 : 127 x 39 x 33
        : 59 x 21 x 7
Zone 4 : 47 x 21 x 7
Zone 5 : 59 x 21 x 7

Figure 3 : Geometry and computational grid for the old design
of the LVAD impeller

Figure 4 : Axial velocity contours at the exit plane of various LVAD impeller design

Pressure
0.3
-0.2
-0.7

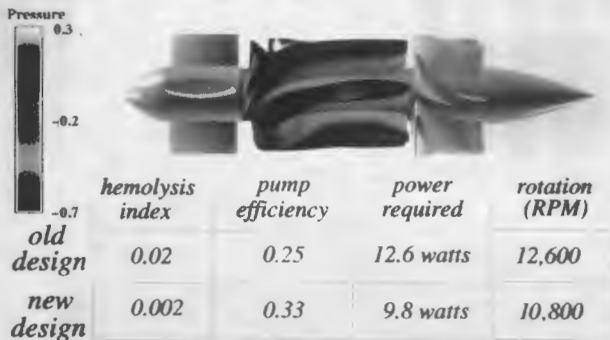|	hemolysis index	pump efficiency	power required	rotation (RPM)
old design	0.02	0.25	12.6 watts	12,600
new design	0.002	0.33	9.8 watts	10,800

Figure 5 : Hub and blade surfaces of the old and new designs of the LVAD impeller are colored by pressure. The table shows clinical results from BCOM

VELOCITY
1.2
0.6
0.0

Figure 6 : Particle traces inside of the new design of the LVAD impeller are colored by velocity magnitude